Internal Report
DESY F1/F33/F39-76/05
October 1976

The Helix Tube Chamber

by

G. Flügge, H. Jensing, A. Marxen, M. Rössler,
H. Schultz, A. Stüben, W. Zimmermann
Deutsches Elektronen-Synchrotron DESY, Hamburg

and

H. Meyer
Gesamthochschule Wuppertal

THE HELIX TUBE CHAMBER

G. Flügge, H. Jensing, A. Marxen,
M. Rössler, H. Schultz, A. Stüben,
W. Zimmermann
Deutsches Elektronen-Synchrotron DESY, Hamburg, Germany

and

H. Meyer
Gesamthochschule Wuppertal, Germany

Abstract

We report on the performance of a 1 m long position sensitive proportional tube. The position coordinate in the direction of the proportional wire is obtained to an accuracy of $\sigma = 2.8$ mm by means of a helical delay line. This proportional chamber is designed to form a large cylindrical detector system.

Introduction

The helix tube chamber is a proportional tube providing a good spatial resolution in the direction of the proportional wire. The position of an ionizing particle passing through this detector is determined by measuring the time difference between the detection of the fast proportional wire signal and the cathode signal, which has to travel along a helical delay line.

Important features of the helix tube chamber are:

- Chambers may be combined to form large area detector systems.
- No cross talk of signals, since neighbouring tubes are decoupled by a grounded outer shielding.
- The chambers are electrically and mechanically separated from each other, so breaking of any high voltage wire affects only one tube, the loss of efficiency is small.
- Simple and inexpensive construction of great mechanical stability.

Operation Principle and Chamber Construction

The operation principle of the helix tube chamber is illustrated in Figure 1. A charged particle passing through the detector gives rise to a fast negative signal on the proportional wire. On the cathode, an inverted signal is obtained by influence as usual in proportional chambers. The cathode of our detector is built in form of a delay line with axis parallel to the proportional wire. The conductors of the delay line are a wire helix and a grounded aluminum foil. The dielectric medium between the conductors, which is responsible for the specific delay-line parameters, is represented by glassfibre-epoxy material forming the wall of the proportional tube.

The signal propagating on the delay line reaches the end of the detector after a time proportional to the distance between particle trajectory and detector end. The position of an event can be determined by measuring the propagation time of the cathode signal along the helix tube chamber. To match reflections, the ends of the helix are terminated with the impedance Z_0 of the delay line. The signals from the proportional wire and the helix provide the start and stop signals for a comparator digitizer, which is read out by a standard CAMAC system. A block diagram of our readout electronics is shown in Figure 2.

Since the cathode of the helix tube chamber is built as an integrated delay line, there are no coupling losses and the cathode signal is comparable to the anode signal.

The delay-line parameters may be calculated with some simple equations.

The capacity per unit length of the helix to good approximation is given by

$$C' = \frac{.1772 \cdot \varepsilon_r}{\frac{2a}{h} + \pi \frac{h}{d}} \quad (pF/cm)$$

where a = distance between helix and shielding (cm),

h = pitch of the helix (cm),

d = diameter of the helix wire (cm),

ε_r = rel. dielectric number of the tube material.

The inductance per unit length is approximately given by

$$L' = 2 \left(\ln \frac{D}{d} + \frac{D^2}{h} \ln \frac{D}{h}\right) \quad (nH/cm)$$

with D = diameter of the helix (cm).

Neglecting the resistance of the helix wire, the impedance and delay time per unit length are

$$Z_o = \sqrt{L'/C'} \quad (\Omega)$$

and

$$t' = \sqrt{L' \cdot C'} \quad (s/cm).$$

The length of the delay line is

$$s = (D + a) \cdot \pi \cdot \frac{l}{h} \quad (cm)$$

with l = length of the proportional tube (cm).

For the total delay of a cathode-signal travelling all along the helix, we get

$$t = t' \cdot s \quad (ns).$$

Table 1 shows the geometrical parameters of our test chamber and a comparison of calculated and measured values for impedance and delay time of the helix. We note a good agreement between calculation and measurement.

Table 1 Test chamber parameters

		calculated	measured
impedance	Z_o	431 Ω	420 Ω
total delay	t	387 ns	375 ns

distance helix to shielding	a	= .65 mm
pitch of the helix	h	= .5 mm
diameter of the helix wire	d	= .2 mm
diameter of the helix	D	=5.9 mm
length of the test chamber	l	= 984 mm
relative dielectric number	ε_r	=4.4

Figure 3 shows a drawing of our test chamber. The construction of the helix tube follows a very simple and cheap procedure. A helix made of 200 µm cu-wire is wound with constant pitch on a metal rod coated with a teflon tube. A woven fibreglass tube is pulled over the helix and moistened with epoxy-adhesive. After hardening of the adhesive, first the metal rod and then the teflon tube can be removed. As proportional wire we use 30 µm gold plated tungsten stretched to a tension of 50 g, mounted on plexiglass endpieces which also provide the gas inlets. Aluminum foil is glued on the outside of the tube to serve as ground potential for the delay line. As an important design feature the grounded shielding has a small slit along the tube. A closed aluminum shielding provides a shortage around the circumference of the tube and generates a contrainductance which, as we found out, deteriorates the pulse shape.

Test Results

The mechanical and electromagnetical properties of our test chamber are listed in Table 1. Positive high voltage was applied to the proportional wire. As operating gas mixture we used 90 % Argon and 10 % Propane. After preamplification by a factor of 4 for the proportional wire signals and a factor of 8 for the delay-line signals the threshold of our readout electronics was set to 5 mV.

Typical signals from anode and cathode of the helix tube chamber are shown in Figure 4. It is seen that the shape of the delay-line signals does not change with distance from the readout side of the helix tube. Cathode signals generated by particles crossing the detector near the readout end have a risetime of 45 ns.

Due to the dispersion of the signals in the electromagnetic transmission line, which is caused by the resistance of the helix wire, the risetime increases to 55 ns at the far end of the detector. The loss of amplitude is about 10 %.

To determine the detection efficiency, the linearity and the position resolution, we used a 250 μ Ci ^{106}Ru-ß-source collimated to 1.5 mm diameter. The electron trajectories through the chamber were defined by a coincidence of two 3 mm diameter scintillation counters placed in front and behind the helix tube.

Figure 5 shows the plateau curve of our helix tube chamber. With the experimental set-up described above we measured a detection efficiency of more than 99.5 % relative to the scintillation counters, with no dependence on the position along the detector.

At an anode voltage of 1410 Volts, the first Geiger pulses appeared in our test chamber. Further increasing of the high voltage resulted in a breakdown at 1550 Volts. In tests with cosmic muons our detector operated without any discharges at anode voltages up to 1700 Volts.

With the Ru source we measured a position resolution of better than σ = 3.7 mm over the whole length of the detector. Fitting the peaks of the position spectrum to Gaussian shape and correcting for the divergence of the electron beam yields a lower limit of σ = 2.3 mm for the position resolution of our test chamber. A best estimate of σ = 2.8 mm is compatible with the full width at half maximum of all observed peaks. The resolution does not change significantly with distance from the readout end of the chamber. Figure 6 shows a position s spectrum over our helix tube chamber, the source being moved in steps of 50 mm.

The nonlinearity of the chamber has been determined by moving the source in steps of 20 mm over 970 mm of the tubelength. The obtained distribution of peak intervalls has a width of σ = 1 mm. The largest deviation from the mean value is 2.3 mm. Both values are well contained in the space resolution of the test chamber. In the direction transverse to the proportional wire, the position resolution is equal to the inner diameter of the tube. The use of two or more displaced layers of helix tube chambers results in 100 % detection efficiency as well as in an improved spatial resolution.

Conclusions

The helix tube chamber offers a good spatial resolution in two dimensions at low expenses. The comparatively small memory time of the delay line (smaller than 400 ns per meter tubelength) makes this proportional tube capable of high counting rates.

We intend to use a cylindrical system of 880 helix tube chambers to determine showerpositions in a 1.2 m diameter barrelshaped lead-scintillator showercounter for the magnetic detector PLUTO. Figure 7 shows a section of this showercounter, which covers a solid angle of .53 · 4π around the interaction point of the electron-positron storagering DORIS. The barrel showercounter consists of two rings segmented into 30 lead-scintillator sandwich modules each. The inner ring has a thickness of 3.6 radiation lengths, the outer ring of 4.3 radiation lengths. In the gap between the two rings, two displaced rings of helix tube chambers localize the z and ϕ coordinates of electromagnetic showers and of high energy particles. The helix chambers are combined to 10 moduls with 88 tubes each.

Acknowledgments

We are grateful to W. Mehrgardt and R. Pforte for the set-up of the CAMAC system and the readout software. We thank H. Ahrens, R. Cyriacks, K. Finke and H. Kock for their help in the construction and in the electronic tests of the helix chambers.

Figure Captions

Fig. 1: Schematic view of the helix tube chamber and principle of operation.

Fig. 2: Block diagram of the readout electronics.

Fig. 3: Drawing of the helix tube chamber.

Fig. 4: Shape of the pulses on anode and cathode of the test chamber as taken with a ^{60}Co source.

Fig. 5: Efficiency plateau curve of the test chamber.

Fig. 6: Position spectrum over the test chamber. A ^{106}Ru source was moved in steps of 50 mm all along the tube.

Fig. 7: A section of the barrel-shaped showercounter for the magnetic detector PLUTO. Two layers of helix tube chambers are situated between two lead-scintillator showercounter rings.

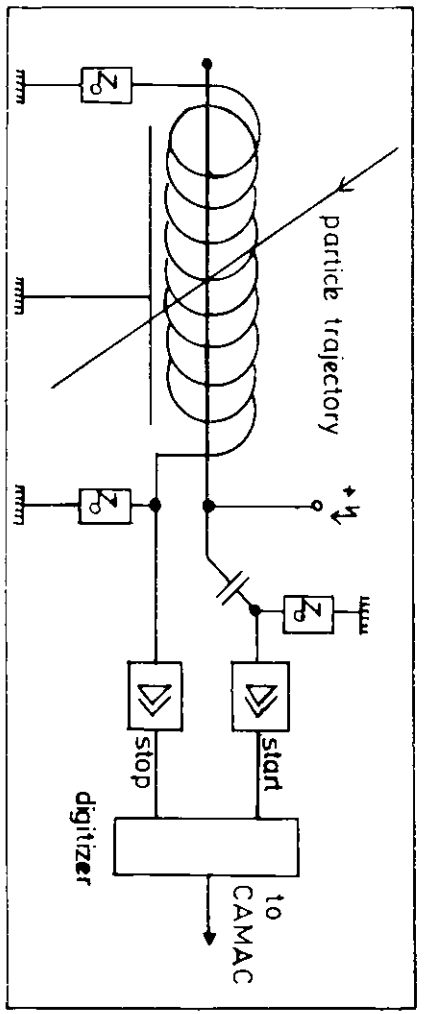

Fig. 1: Operation principle

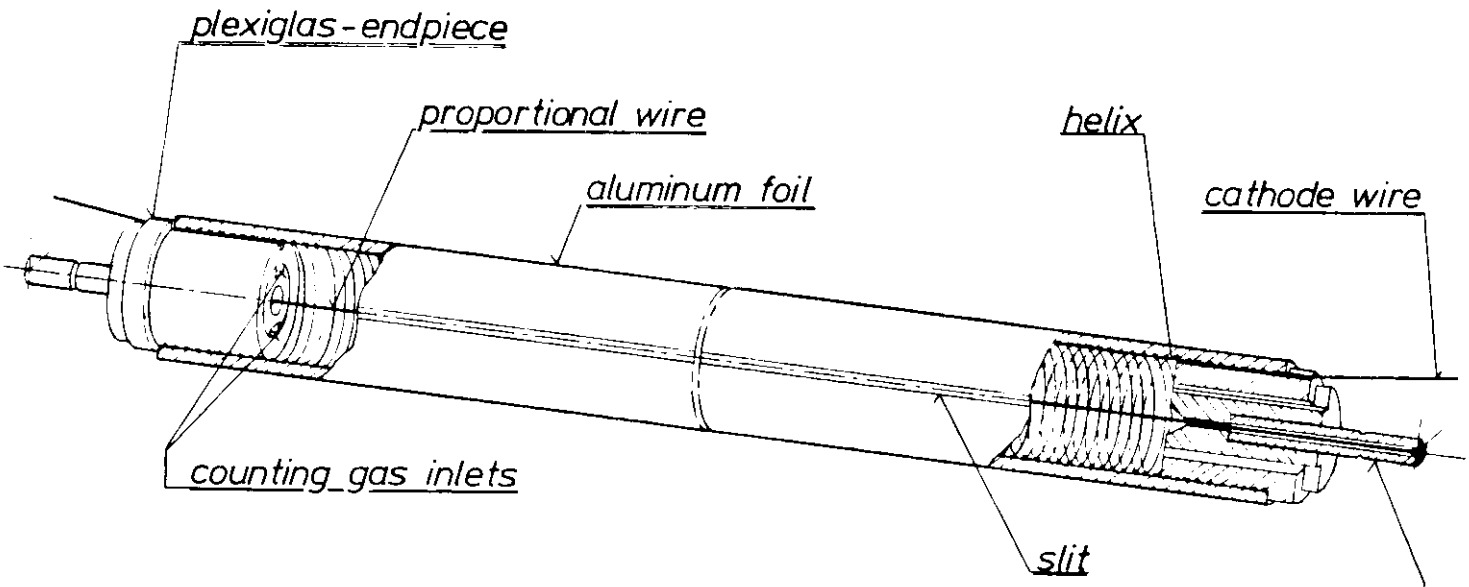

FIG.3:Helix Tube Chamber

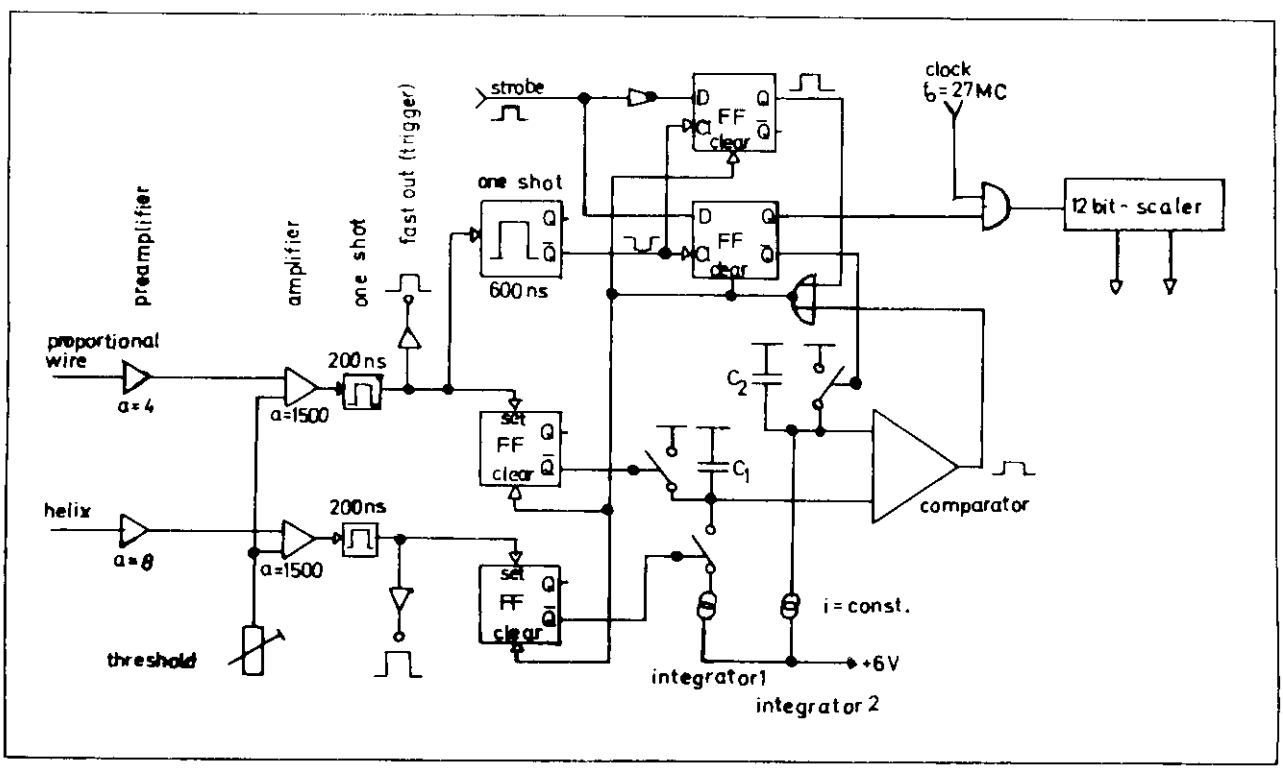

Fig.2:Readout electronics

a)

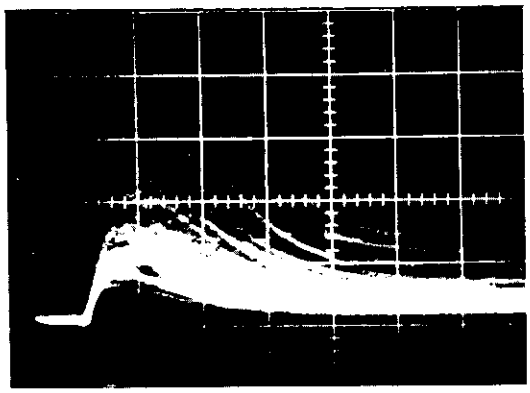

b)

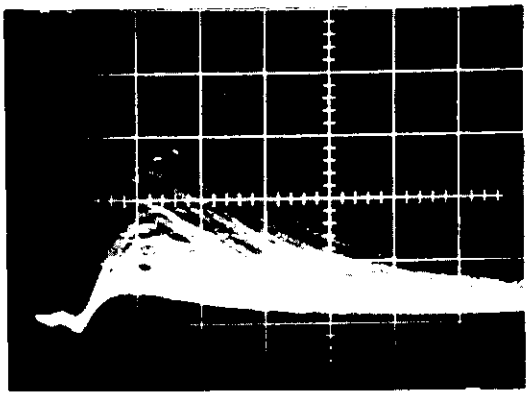

c)

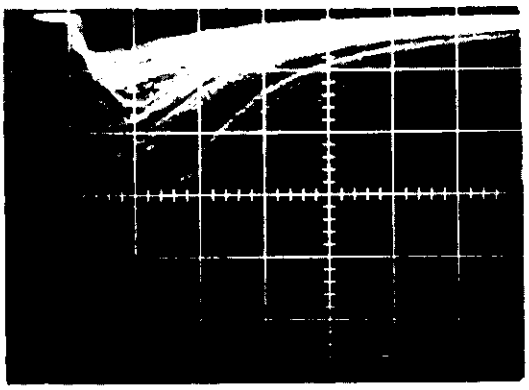

a) delayline signals, source near to the readout-end

b) delayline signals, source far from the readout-end

c) proportional wire signals

Fig. 4: Pulse shapes. Vertical scale, 20 mV/div., horizontal scale, 100 nsec/div.

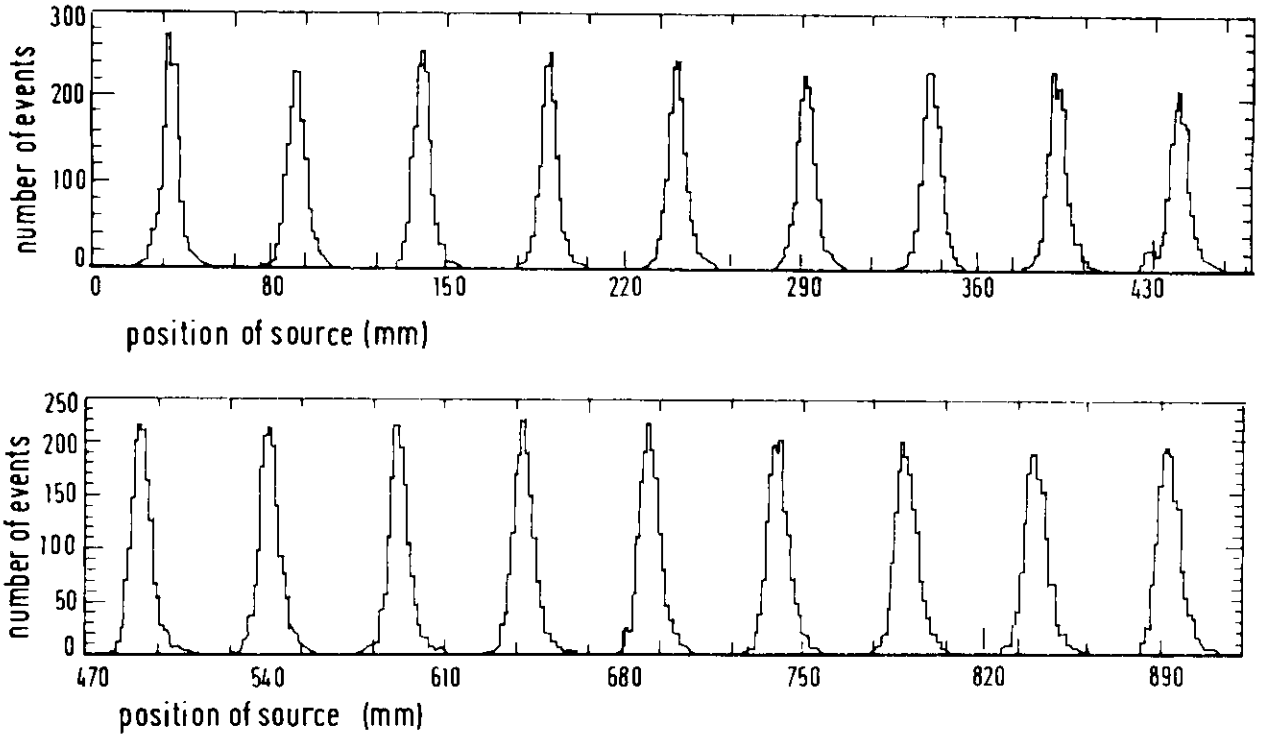

Fig. 6 : Position resolution measured with a ^{106}Ru source.
Distance between peaks = 50mm

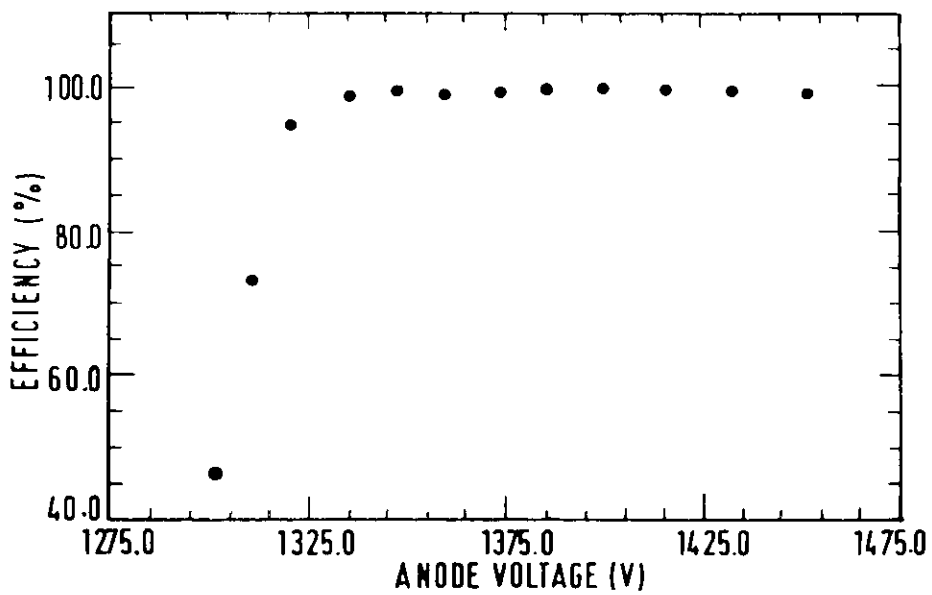

Fig. 5 PLATEAU CURVE

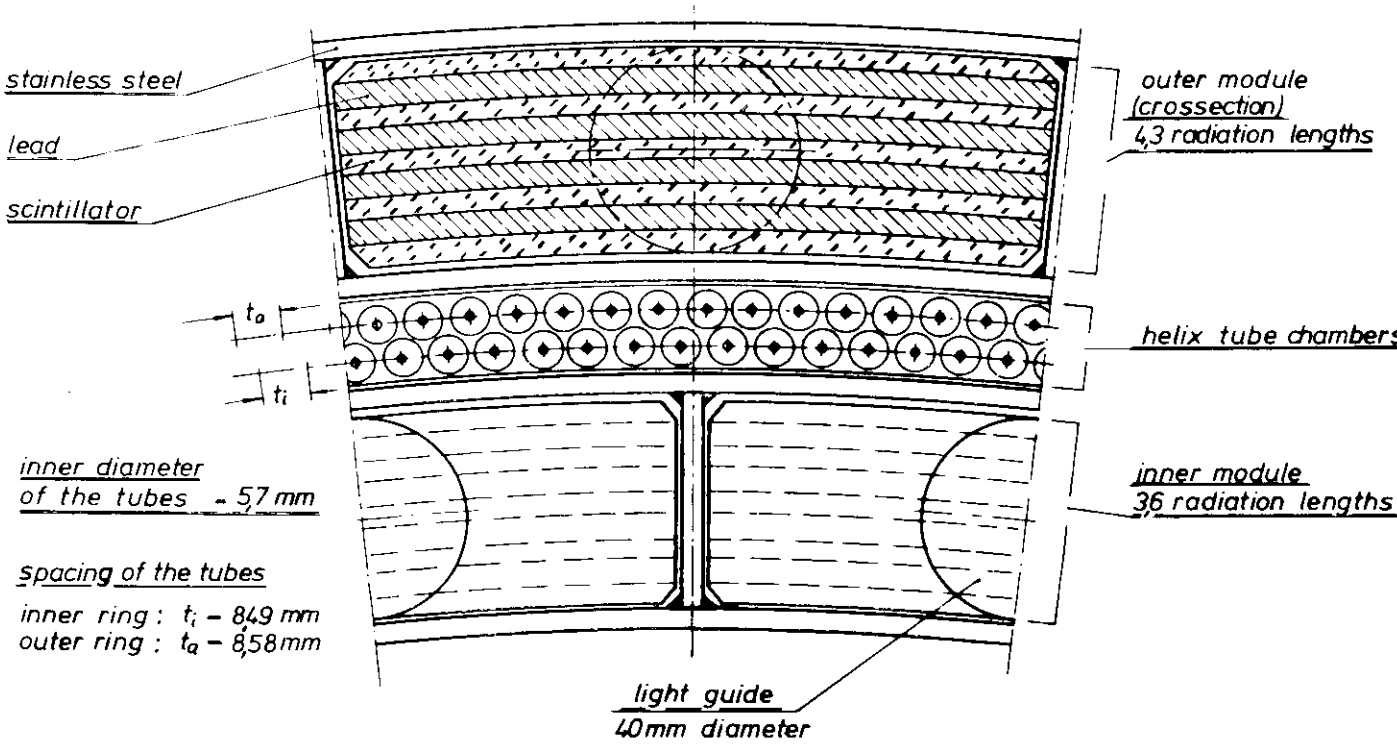

Fig: 7

Section of the barrel showercounter